

The added value of abnormal regional myocardial function for risk prediction in arrhythmogenic right ventricular cardiomyopathy

Feddo P. Kirkels ^{1,2,3,4}, Christine Rootwelt-Norberg ^{4,5}, Laurens P. Bosman ¹, Eivind W. Aabel^{4,5}, Steven A. Muller^{1,2}, Anna I. Castrini^{4,5}, Karim Taha ¹, Nick van Osta ³, Øyvind H. Lie⁴, Folkert W. Asselbergs^{6,7}, Joost Lumens ³, Anneline S.J.M. te Riele^{1,2}, Nina E. Hasselberg^{4,5}, Maarten J. Cramer¹, Kristina H. Haugaa ^{4,5†}, and Arco J. Teske ^{1*†}

¹Division of Heart and Lungs, Department of Cardiology, University Medical Centre Utrecht, Heidelberglaan 100, Utrecht 3582 CX, The Netherlands; ²Netherlands Heart Institute, Utrecht, The Netherlands; ³Department of Biomedical Engineering, Cardiovascular Research Institute Maastricht (CARIM), Maastricht University, Maastricht, The Netherlands; ⁴ProCardio Centre for Innovation, Department of Cardiology, Oslo University Hospital, Rikshospitalet, Oslo, Norway; ⁵Institute of Clinical Medicine, Faculty of Medicine, University of Oslo, Oslo, Norway; ⁶Department of Cardiology, Amsterdam University Medical Centre, University of Amsterdam, Amsterdam, The Netherlands; and ⁷Health Data Research UK and Institute of Health Informatics, University College London, London, UK

Received 15 May 2023; accepted 13 July 2023; online publish-ahead-of-print 20 July 2023

Aims

A risk calculator for individualized prediction of first-time sustained ventricular arrhythmia (VA) in arrhythmogenic right ventricular cardiomyopathy (ARVC) patients has recently been developed and validated (www.ARVCrisk.com). This study aimed to investigate whether regional functional abnormalities, measured by echocardiographic deformation imaging, can provide additional prognostic value.

Methods and results

From two referral centres, 150 consecutive patients with a definite ARVC diagnosis, no prior sustained VA, and an echocardiogram suitable for deformation analysis were included (aged 41 ± 17 years, 50% female). During a median follow-up of 6.3 (interquartile range 3.1–9.8) years, 37 (25%) experienced a first-time sustained VA. All tested left and right ventricular (LV and RV) deformation parameters were univariate predictors for first-time VA. While LV function did not add predictive value in multivariate analysis, two RV deformation parameters did; RV free wall longitudinal strain and regional RV deformation patterns remained independent predictors after adjusting for the calculator-predicted risk [hazard ratio 1.07 (95% CI 1.02–1.11); $P = 0.004$ and 4.45 (95% CI 1.07–18.57); $P = 0.040$, respectively] and improved its discriminative value (from C-statistic 0.78 to 0.82 in both; Akaike information criterion change > 2). Importantly, all patients who experienced VA within 5 years from the echocardiographic assessment had abnormal regional RV deformation patterns at baseline.

Conclusions

This study showed that regional functional abnormalities measured by echocardiographic deformation imaging can further refine personalized arrhythmic risk prediction when added to the ARVC risk calculator. The excellent negative predictive value of normal RV deformation could support clinicians considering the timing of implantable cardioverter defibrillator implantation in patients with intermediate arrhythmic risk.

* Corresponding author. E-mail: AJ.Teske-2@umcutrecht.nl

† These authors shared last authorship to this study.

© The Author(s) 2023. Published by Oxford University Press on behalf of the European Society of Cardiology.

This is an Open Access article distributed under the terms of the Creative Commons Attribution-NonCommercial License (<https://creativecommons.org/licenses/by-nc/4.0/>), which permits non-commercial re-use, distribution, and reproduction in any medium, provided the original work is properly cited. For commercial re-use, please contact journals.permissions@oup.com

patients in this process, a multimodality risk calculation tool was published in 2019⁴ and its utility has been replicated in multiple independent cohorts.^{5–8} In addition, a recent study validated the risk calculator as an accurate tool to repeatedly calculate arrhythmic risk during follow-up.⁹

Visualization of the structural disease substrate is an important part of arrhythmic risk stratification in ARVC. RV ejection fraction (RVEF), measured by cardiac magnetic resonance (CMR) imaging, is currently the only imaging parameter included in the ARVC risk calculator. While global systolic function of the RV is well reflected in the EF, we know that life-threatening VA can already occur early in the disease. In this stage, fibrofatty replacement of myocardial tissue leads to regional wall motion abnormalities while the global systolic function is preserved. Echocardiographic deformation imaging has developed as a more sensitive method for detection of regional abnormalities in myocardial function. Regional deformation abnormalities have been associated with arrhythmia in ARVC patients, whereby especially negative predictive value of normal deformation was high.^{10–13} Although results of previous studies were promising, the added predictive value of echocardiographic deformation imaging should be tested in a multimodality approach and on top of current clinical practice. The purpose of this study was to test the predictive value of echocardiographic deformation imaging in a primary prevention cohort of patients with ARVC and to further improve arrhythmic risk stratification by investigating whether it has prognostic value independent of the ARVC VA risk calculator.

Methods

Study design and population

We included consecutive patients with definite ARVC who presented to the University Medical Centre Utrecht in the Netherlands and the Oslo University Hospital in Norway up until 1 January 2023. These patients were partially included in previous studies.^{10,11,14,15} ARVC diagnosis was defined according to the 2010 Task Force Criteria (TFC).¹⁶ Patients with previous myocardial infarction or congenital heart disease were excluded. Date of inclusion was defined as the date of echocardiographic examination closest to date of diagnosis and available for performing deformation imaging. Patients with VA prior to baseline evaluation were excluded. The study was approved by both local institutional ethics review boards and complies with the Declaration of Helsinki.

Data collection

For each patient, baseline demographics, treatment with antiarrhythmic medication, and presence of an ICD were recorded. Electrocardiogram (ECG), Holter, and CMR data from the study closest to baseline echocardiography and prior to occurrence of primary outcome were used. The seven variables included in the ARVC risk calculator (www.ARVCrisk.com) were collected independently in each centre according to uniform definitions and included age at diagnosis, sex, recent syncope (<1 year ago), number of inferior/anterior leads with T-wave inversion, non-sustained ventricular tachycardia (NSVT), 24-h premature ventricular complex (PVC) count, and RVEF measured by CMR. All genetic variants reported were adjudicated according to the American College of Medical Genetics and Genomics guidelines.¹⁷

The echocardiographic deformation imaging protocol was previously described in more detail.^{12,15} We used a GE Vivid 7, E9, or E95 scanner and loops were stored for post-processing with EchoPac version 203 (GE HealthCare, Horten, Norway). All measurements were performed by a single observer according to the current guidelines^{18,19} and blinded to clinical outcome. Data on inter- and intra-observer variability are provided in [Supplementary data online, Table S1](#). Myocardial deformation was assessed in three apical views of the left ventricle (LV) and in the RV-focused four-chamber view. Predictive value of the following five deformation parameters was tested: LV global longitudinal strain (GLS), LV and RV mechanical dispersion (LVMD and RVMD, respectively), RV free wall longitudinal strain (RV_{FWLS}), and regional RV deformation patterns. LV GLS was

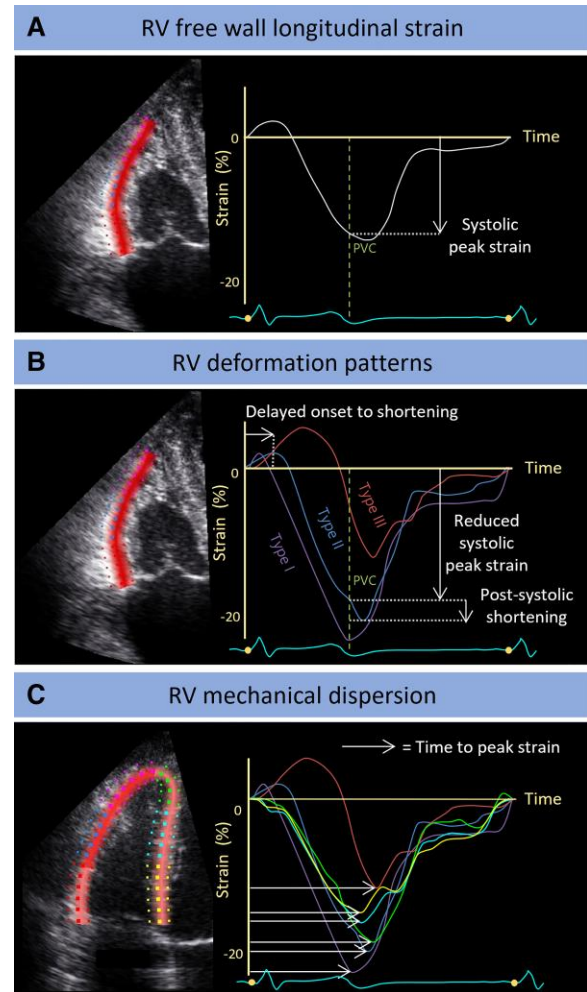


Figure 1 Echocardiographic deformation imaging in an RV-focused view. (A) RV_{FWLS} was calculated as the systolic peak strain from the averaged regional RV free wall deformation characteristic. (B) Based on predefined criteria, a division into three different deformation patterns was identified in all three segments of the RV lateral wall.¹⁵ Type I is normal deformation. Types II and III are abnormal deformation, whereby Type II is characterized by delayed onset of shortening, reduced systolic peak strain, and minor post-systolic shortening; Type III is characterized by little or no systolic peak strain, predominantly systolic stretching, and major post-systolic shortening. (C) For RV mechanical dispersion, a six-segment model of the RV was used, including both the lateral wall and the interventricular septum. It was calculated as the SD of the segmental time intervals from onset Q/R on the surface ECG to peak negative strain and expressed in ms.¹² PV, pulmonic valve closure; RV, right ventricular.

calculated as the peak negative strain from the averaged regional 16-segment LV model.¹⁸ Mechanical dispersion was calculated as the standard deviation (SD) of the segmental time intervals until maximum shortening of 16 segments in the LV and 6 segments in the RV.¹² RV_{FWLS} was defined as the peak negative strain from the averaged regional RV free wall deformation curve. Deformation patterns were analysed in the basal, mid, and apical segments of the RV free wall. The RV deformation pattern was classified as normal if the pattern was normal in all three segments and abnormal if at least one segment showed abnormal deformation (Figure 1).^{10,15}

Missing data

Missing data were assumed to be missing at random and imputed using multiple imputation with chained equations as described previously.⁴ The multiple imputation model included all pre-specified predictors, proband status and genotype together with the outcome, and cumulative baseline hazard estimation.^{20,21} A total of 25 imputed data sets were generated, and the final inference estimations were combined using Rubin's rules.²²

All covariates of the ARVC risk calculator and the deformation imaging variables had <5% missingness, except for 24-h PVC count (11%) and RVEF by CMR (19%). Complete case analyses without imputation and 24-h PVC count and RVEF were performed as sensitivity analyses (see [Supplementary data online, Table S2](#)).

Study outcomes

The primary outcome of the study was first sustained VA after TFC-based ARVC diagnosis. In accordance with the published ARVC risk calculator, sustained VA was defined as sustained ventricular tachycardia lasting ≥ 30 s at ≥ 100 bpm, aborted cardiac arrest, or appropriate ICD therapy. Incident heart transplantation, cardiovascular mortality, and all-cause mortality were also recorded during follow-up. Follow-up duration was defined as the time interval between baseline echocardiography and VA or censoring, which was defined as last clinical visit if lost to follow-up or 1 January 2023.

Statistical analysis

Analyses were performed with RStudio (v. 2022.12.0, Boston, USA) and Stata (v. 16.0, StataCorp, Texas, USA). Continuous variables were expressed as mean with SD or median with interquartile range (IQR) and compared using independent sample *t*-test or Mann–Whitney *U* test. Categorical variables were presented as frequencies (%) and compared using the Fisher exact test. VA-free survival probability was estimated using the Kaplan–Meier method and Cox proportional hazard regression analysis. For Kaplan–Meier analysis of continuous variables, categorization was based on threshold regression analysis. All deformation imaging variables were subjected to linearity and proportional hazards assumption testing criteria. *P*-values were two sided, and values <0.05 were considered significant.

Model testing

The overall discriminative performance of the ARVC risk calculator was measured using the optimism-corrected Harrell's *C*-statistic. The 5-year risk of sustained VA for an individual patient as per the published model was calculated using the following equation⁴:

$$5 \text{ year VA risk} = 1 - 0.84 \exp(\text{PI}),$$

where the prognostic index (PI) was calculated according to the equation:

$$\begin{aligned} \text{PI} = & \text{male sex} * 0.49 - \text{age} * 0.022 + \text{cardiac syncope} * 0.66 \\ & + \text{NSVT} * 0.81 + \ln(24\text{-h PVC count}) * 0.17 + \text{TWI} * 0.11 \\ & - \text{RVEF} * 0.025. \end{aligned}$$

Based on the 5-year risk of sustained VA, patients were stratified into low-risk (<5%), intermediate-risk (5–25%), and high-risk (>25%) subgroups. Of note, the baseline hazard for 5-year prediction (0.84) has been corrected since the initial publication in 2019.²³

To assess the predictive ability of deformation imaging for VA events, Cox proportional hazards models of VA events were fitted to deformation imaging results. The strongest deformation imaging parameters were identified by stepwise backward selection in a multivariate Cox proportional hazards model and tested for prognostic value independent of the ARVC risk calculator PI (incorporated as a fixed offset variable). Model discriminations were assessed using a non-parametric concordance-based *C*-statistic. The

added value of deformation imaging to the ARVC risk calculator for predicting VA events was assessed by comparison of optimism-corrected *C*-statistics. The Akaike information criterion (AIC) was estimated for the risk models, for which a reduction of >2 was considered a significant improvement.

Results

Clinical characteristics

From 439 eligible patients, 130 were excluded due to prior VA, 146 were family members carrying a (likely-)pathogenic genetic variant who did not fulfil a definite TFC diagnosis, and 13 were excluded due to various other reasons as shown in [Supplementary data online, Figure S1](#). Hence, the final cohort consisted of 150 patients ([Table 1](#); see [Supplementary data online, Table S3](#) for data per centre) with a definite ARVC diagnosis and no prior VA who underwent echocardiographic deformation imaging. Mean age at baseline echocardiography was 41 ± 17 years; 75 (50%) patients were male, and 51 (34%) were proband. Median follow-up duration was 6.3 (IQR 3.1–9.8) years. The majority of patients (86%) were carriers of a (likely-)pathogenic genetic variant, of which mutations in the *PKP2* gene (66%) were most prevalent.

Outcomes

Thirty-seven patients (25%) experienced the primary outcome of first sustained VA after a median follow-up of 2.9 years (IQR 0.9–6.0) ([Figure 2](#); see [Supplementary data online, Figure S2](#) for data per centre). The corresponding annual event rate of the primary endpoint was 3.6% (95% CI 2.6–5.0%). The most common primary endpoint was appropriate ICD therapy ($n = 26$, 70%), followed by sustained VA ($n = 10$, 27%) and sudden cardiac arrest ($n = 1$, 3%). At the last follow-up, half of the patients ($n = 75$, 50%) had received an ICD. Eight (5%) patients had died of mostly non-cardiac cause ($n = 6$, 4%), and three (2%) had undergone heart transplantation.

Deformation imaging and incidence of VA

One patient was excluded because of insufficient image quality for any deformation analyses. Of included patients, LV deformation imaging was feasible in 146 patients (97%) and RV deformation imaging in 148 patients (99%). For the LV deformation parameters, LV GLS was worse in patients who later experienced VA, while LVMD was not ([Table 1](#)). All three RV deformation parameters (RV_{FVW}LS, RVMD, and RV deformation pattern) were more abnormal in patients with VA during follow-up. Regional RV deformation patterns were abnormal (i.e. Type II or Type III) at baseline in 94% of patients with VA anytime during follow-up against 56% in patients without VA. Moreover, all patients who experienced the primary outcome within 5 years from the echocardiographic assessment had abnormal RV deformation patterns at baseline. Nevertheless, the positive predictive value of an abnormal RV deformation pattern for VA within 5 years was low with 0.41 [95% confidence interval (CI) 0.32–0.50]. The worst outcome was seen in patients with the most abnormal type III deformation pattern ([Figure 3B](#)). For the Kaplan–Meier plot of RV_{FVW}LS ([Figure 3A](#)), threshold regression analysis identified two optimal cut-offs for increased arrhythmic risk (–24% and –17%).

Univariate survival analysis showed increased hazard of VA occurrence for all tested deformation parameters, as expressed by hazard ratios ([Table 2](#)).

Deformation imaging in personalized risk prediction

Discriminative value of the current ARVC risk calculator model was good in this cohort with a *C*-statistic of 0.78 (95% CI 0.71–0.86),

Table 1 Baseline characteristics of ARVC patients without and with sustained VA during follow-up

	All (N = 150)	No VA (n = 113)	VA (n = 37)	P-value
Demographics				
Age at echocardiography, yrs	41.3 ± 17.1	41.8 ± 17.3	39.8 ± 16.8	0.558
Male	75 (50)	54 (48)	21 (57)	0.449
Proband	51 (34)	30 (27)	21 (57)	0.002
Genetic status				
(Likely-)pathogenic variant	129 (86)	102 (90)	27 (73)	0.018
PKP2	99 (66)	74 (66)	25 (68)	
DSP	3 (2)	3 (3)	0 (0)	
DSG2	5 (3)	5 (4)	0 (0)	
PLN	18 (12)	16 (14)	2 (5)	
Multiple	1(1)	1 (1)	0 (0)	
Other	3 (2)	3 (3)	0 (0)	
Clinical history				
Any cardiac symptoms	105 (70)	73 (65)	32 (87)	0.021
Recent cardiac syncope	12 (8)	2 (2)	10 (27)	<0.001
Treatment at baseline				
ICD	19 (13)	12 (11)	7 (19)	0.302
Anti-arrhythmic drugs	24 (16)	18 (16)	6 (16)	1
Beta-blockers	45 (30)	33 (30)	12 (32)	0.893
Clinical phenotype				
Total TFC score	5 (4–6)	5 (4–6)	7 (5–8)	<0.001
Age at diagnosis	40.7 ± 16.7	41.3 ± 16.6	38.8 ± 17.1	0.436
ECG				
TWI in ≥3 precordial leads	57 (38)	38 (34)	19 (51)	0.078
TWI in ≥2 inferior leads	22 (15)	14 (12)	8 (22)	0.185
PVC count per 24h	497 (48–2322)	281 (31–1496)	894 (757–7884)	<0.001
NSVT	67 (45)	46 (41)	21 (57)	0.141
CMR (n = 141)				
RVEF, %	46 ± 10	48 ± 9	39 ± 10	<0.001
RVEDVi, ml	109 ± 29	105 ± 29	125 ± 24	0.002
LVEF, %	54 ± 9	54 ± 8	52 ± 10	0.387
LGE	23 (20)	16 (18)	7 (25)	0.419
Traditional echocardiography				
LVEF, %	55 ± 8	55 ± 7	53 ± 12	0.216
RVFAC, %	39 ± 9	40 ± 9	35 ± 8	0.017
RVOT, mm	35 ± 7	34 ± 6	37 ± 7	0.058
Echocardiographic deformation imaging				
LV GLS, %	-18.2 ± 3.2	-18.7 ± 2.5	-16.7 ± 4.3	0.001
LVMD, ms	38 (31–47)	38 (30–46)	42 (36–49)	0.107
RV _{F_W} LS, %	-19.5 ± 7.0	-21.0 ± 6.3	-15.0 ± 6.9	<0.001
RVMD, ms	33 (23–44)	30 (21–43)	43 (29–67)	0.003
RV deformation pattern abnormal	97 (66)	63 (56)	34 (94)	<0.001
Type I	51 (35)	50 (45)	2 (6)	
Type II	65 (44)	50 (45)	15 (42)	
Type III	32 (22)	13 (12)	19 (53)	

Values are n (%), mean ± SD or median (25th and 75th percentiles) according to the distribution of normality.

ARVC, arrhythmogenic right ventricular cardiomyopathy; CMR, cardiac magnetic resonance; DSG2, desmoglein-2; DSP, desmoplakin; EDVi, end diastolic volume indexed; EF, ejection fraction; FAC, fractional area change; GLS, global longitudinal strain; LGE, late gadolinium enhancement; LV, left ventricular; MD, mechanical dispersion; NSVT, non-sustained ventricular tachycardia; PKP2, plakophilin-2; PVC, premature ventricular complex; RV, right ventricular; RV_{F_W}LS, right ventricular free wall longitudinal strain; RVOT, right ventricular outflow tract; TFC, Task Force Criteria; TWI, T-wave inversion; VA, ventricular arrhythmia.

consistent with prior results.⁴ The strongest predictors of VA among the deformation parameters were RV_{FWLS} , abnormal RV deformation pattern, and LV GLS. Incremental predictive value was found when adding RV_{FWLS} or abnormal RV deformation pattern to the risk calculator. Adding LV GLS, however, did not seem to improve prediction of VA (Table 3). The resulting adjusted HR was 1.07 (95% CI 1.02–1.11, $P = 0.004$) per % worsening of RV_{FWLS} and 4.45 (95% CI 1.07–18.57, $P = 0.040$) in case of an abnormal regional deformation pattern. Optimism-corrected C-statistics were higher when RV_{FWLS} or RV deformation pattern was added to the model (in both cases 0.82; 95% CI 0.75–0.88). Also, both RV parameters reduced the model AIC by >2, which was not the case for LV GLS.

The intermediate arrhythmic risk subgroup (5-year VA risk 5–25% as per the ARVC risk calculator) consisted of 73 patients. In this subgroup, no events occurred in the 28 patients who had normal regional RV deformation patterns. In the seven intermediate-risk patients who did experience VA during follow-up, we observed abnormal regional RV deformation patterns, resulting in a specificity of 0.41 (95% CI 0.31–0.57) and a positive predictive value of 0.16 (95% CI 0.14–0.19).

Discussion

In this study, we showed that echocardiographic deformation imaging can further refine personalized arrhythmic risk prediction when added to the ARVC risk calculator. Both abnormal regional RV deformation patterns and RV_{FWLS} as a continuous indicator of RV function showed independent predictive value on top of the risk calculator and improved its discriminative value. Measures of LV deformation, on the other hand, did not add predictive value in this cohort. Importantly, all patients who experienced VA within 5 years from the echocardiographic assessment showed abnormal RV deformation patterns at baseline.

Risk stratification in patients with ARVC

Arrhythmic risk prediction is a central part of clinical management of ARVC patients, in order to determine if and when an ICD is warranted. Especially in this disease, risk prediction is challenging, since life-threatening arrhythmias can already occur early in the disease.² Predictors of unfavourable outcome that were identified over the

past decades were recently summarized in a meta-analysis²⁴ and subsequently used for the development of a multimodality risk calculation tool.⁴ This published ARVC risk calculator (www.ARVCrisk.com), which aims to predict the 5-year risk of first sustained VA in patients with definite ARVC, has since been validated in different settings and showed superior performance when compared with existing risk stratification algorithms.^{5–8} In the current cohort, annual event rate was slightly lower compared with the initial risk calculator study⁴ [3.6% (95% CI 2.6–5.0) vs. 5.6% (95% CI 4.7–6.6)], which may be caused by a larger proportion of diagnosed family members in the current cohort, identified through cascade genetic testing. Still, the discriminative value was comparable [0.78 (95% CI 0.71–0.86) vs. 0.77 (95% CI 0.73–0.81)].

Deformation imaging in ARVC arrhythmic risk stratification

Echocardiography has an important role in the diagnosis and follow-up of ARVC patients. However, traditional echocardiographic parameters, such as RV fractional area change and RV outflow tract diameter, may lack sensitivity with regard to detection of early disease substrates.^{4,25,26} Over the past two decades, echocardiographic deformation imaging has evolved into a sensitive method to detect regional abnormalities in myocardial function, reflecting structural disease manifestation in ARVC.^{26–28} Distinct abnormalities in regional myocardial function have been identified, which were associated with disease severity. These regional deformation patterns with delayed onset to shortening, reduced peak strain, and post-systolic shortening (Figure 1) most likely reflect pathologic changes on tissue level that form the substrate for VA.¹⁵ An exploratory study sought to explain these specific deformation types by computer simulation using the CircAdapt model. Indeed, loss in contractility and increase in local myocardial stiffness characterized the regional function abnormalities. Studies consistently showed that the first and most severely affected area was the subtricuspid region of the RV lateral wall,^{10,15,29} a well-known predilection site for the earliest disease manifestation of ARVC.³⁰ Echocardiographic deformation imaging is well suited to evaluate this specific region. Of interest, deformation abnormalities appear already early in the development of this disease and remain stable or progress over time.^{29,31} These observations and modelling data

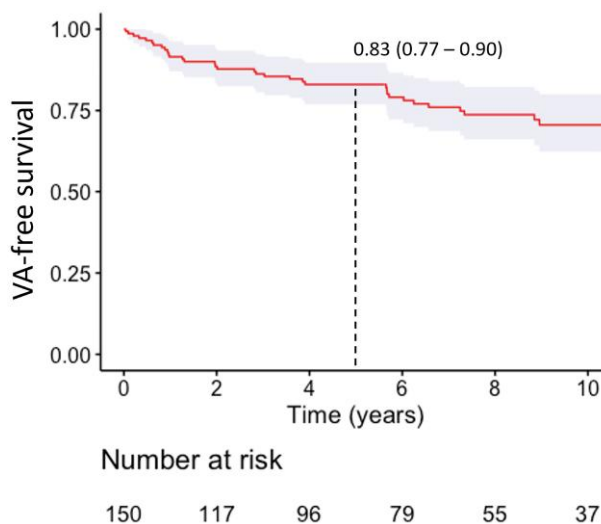


Figure 2 Kaplan–Meier estimate of VA free survival for patients with ARVC without prior sustained VA. Dotted line represents cumulative 5-year survival. VA, ventricular arrhythmia.

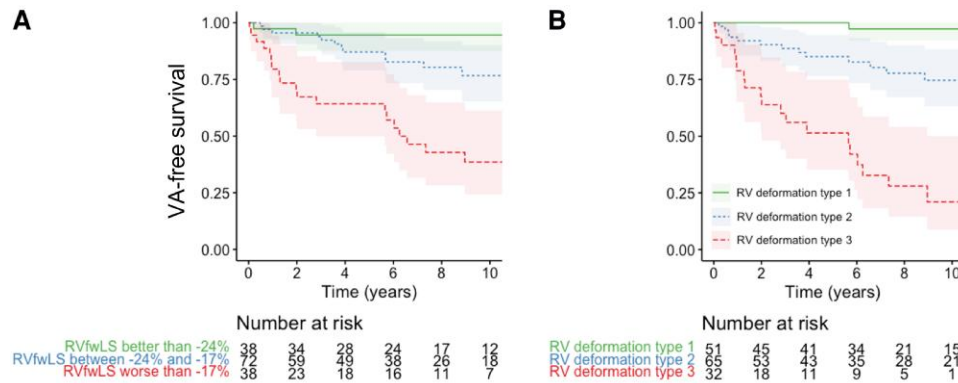


Figure 3 VA free survival in presence of abnormal RV function measured by deformation imaging. (A) When dividing RV_{FWLS} into three groups, a clear difference in VA-free survival was seen. (B) A normal RV deformation pattern (Type I) was associated with excellent negative predictive value (0.96, 95% CI 0.87–0.99). Especially the most abnormal Type 3 deformation was associated with worse outcome. RV, right ventricular; VA, ventricular arrhythmia.

Table 2 Associations between deformation parameters and first sustained VA

	HR (95% CI)	P-value	
LV GLS	1.20 (1.10–1.31)	<0.001	per % worsening
LVMD (ln)	2.73 (1.07–6.98)	0.036	per ln(ms) increase
RV _{FWLS}	1.12 (1.08–1.17)	<0.001	per % worsening
RVMD (ln)	3.09 (1.73–5.53)	<0.001	per ln(ms) increase
RV deformation pattern	10.94 (2.63–45.56)	<0.001	when abnormal

HRs are presented with 95% CIs. Since linearity and proportional hazards assumption testing criteria showed signs of non-linearity for mechanical dispersion, the timing variables LVMD and RVMD were subjected to log transformation. CI, confidence interval; HR, hazard ratio; GLS, global longitudinal strain; LV, left ventricular; MD, mechanical dispersion; RV, right ventricular; RV_{FWLS}, right ventricular free wall longitudinal strain; VA, ventricular arrhythmia.

indicate that this specific functional assessment might be of incremental value in predicting VA, since it seems to reflect the microscopic alterations that form the substrate for re-entry tachycardia. Indeed multiple indicators of myocardial deformation have been associated to VA.^{10–13} In a previous primary prevention study including both ARVC patients and family members at risk, both LVMD and RV_{FWLS} were strong predictors of arrhythmic outcome.¹¹ In a combined cohort with patients from our two centres, especially negative predictive value of normal regional deformation patterns for prior VA (98%) was high.¹⁰ The current prospective study is unique since it included only patients with a definite TFC diagnosis, which explains the high prevalence of abnormal regional RV deformation patterns (66%). Importantly, it confirmed the high negative predictive value of normal deformation, since all patients with VA within 5 years from baseline evaluation already showed regional abnormalities in the RV. In line with previous ARVC studies, the

subtricuspid was consistently first and most severely affected. Up to now, added value of deformation imaging has never been tested on top of current clinical practice. The multimodality ARVC risk score,⁴ a validated clinical risk prediction tool guiding management and ICD necessity, created this opportunity.

Deformation imaging added to the ARVC risk calculator

In a multivariate model, RV deformation patterns and RV_{FWLS} were the strongest independent predictors of first sustained VA. The superiority of RV parameters was not surprising given the fact that patients were selected by the RV-focused 2010 TFC and mostly PKP2 variant carriers were included, who typically present with the classical right dominant ARVC phenotype. Previous papers showed that the ARVC risk calculator performs well in PKP2-dominated cohorts, while for patients with a different genetic background, incorporation of measures of LV function might be important.^{8,32}

When integrated with the ARVC risk calculator, both indices of regional RV deformation still showed independent prognostic value. Models that combined the ARVC risk calculator-predicted risk with regional RV deformation patterns or RV_{FWLS} were superior at predicting VA compared with either of these predictors alone. This confirms our hypothesis that inclusion of measures of regional RV function can improve arrhythmic risk prediction in ARVC.

Clinical implications

This was the first study showing added value of deformation imaging in a clinical practice-based, multimodality approach. Both RV deformation patterns and RV_{FWLS} were able to refine risk stratification when added to the existing ARVC risk calculator. Especially negative predictive value of deformation imaging was high; none of the patients with normal regional RV deformation patterns at baseline experienced VA within 5 years from the echocardiogram. With a two-step approach, this additional stratification tool can probably be of greatest use in the intermediate arrhythmic risk group (5–25% at 5 years) as predicted by the ARVC risk calculator. In these patients, the timing of ICD implantation is the most challenging. Normal RV deformation could in this case reassure both clinician and patient in a watchful waiting strategy regarding ICD implantation (*Structured Graphical Abstract*). While echocardiographic deformation imaging has shown the ability to reveal early signs

Table 3 The added value of deformation imaging for personalized arrhythmic risk prediction in ARVC

	Adjusted HR (95% CI)	P-value	C-statistic (95% CI)	AIC
Risk calculator model	0.78 (0.71–0.86)	299.2
+RV _{FW} LS per % worsening	1.07 (1.02–1.11)	0.004	0.82 (0.75–0.88)	–7.2
+RV deformation abnormal	4.45 (1.07–18.57)	0.040	0.82 (0.75–0.88)	–6.6
+LV GLS per % worsening	1.07 (0.98–1.18)	0.138	0.79 (0.72–0.86)	–1.3

HRs are adjusted for the calculator-predicted risk. HR and optimism-corrected C-statistic are presented with 95% CIs.

AIC, Akaike information criterion; ARVC, arrhythmogenic right ventricular cardiomyopathy; CI, confidence interval; HR, hazard ratio; LV GLS, left ventricular global longitudinal strain; RV, right ventricular; RV_{FW}LS, right ventricular free wall longitudinal strain.

of disease associated with arrhythmic outcome in multiple genetic cardiomyopathies,^{27,33,34} predictive value when added to clinical risk prediction tools in these diseases is yet to be investigated.

Limitations

Due to the high prevalence of patients with (likely-)pathogenic variants in the *PKP2* gene (66%), generalizability to patient populations with other dominating variants is uncertain. A genotype-specific approach might improve predictive value especially for non-*PKP2* patients, as pointed out in a recent validation of the ARVC risk calculator,⁸ but is hindered by lack of power.

The feasibility of echocardiographic deformation imaging depends on image quality. With >95% for both LV and RV deformation imaging, feasibility was high in the ARVC cohorts included in this study. If centres do not routinely perform dedicated RV-focused images, feasibility may drop.

Last, this was an observational study with inherent limitations by study design. Validation in an external cohort will be important for the clinical implementation of integrating deformation imaging with the ARVC risk calculator.

Conclusion

This study showed that inclusion of regional abnormalities in RV function can further refine personalized arrhythmic risk prediction in ARVC. Both regional deformation patterns and longitudinal strain of the RV free wall improved prediction of arrhythmic outcome beyond the ARVC risk calculator. With a two-step approach, the excellent negative predictive value of normal RV deformation could support clinicians considering the timing of ICD implantation in patients with intermediate arrhythmic risk.

Supplementary data

Supplementary data are available at *European Heart Journal - Cardiovascular Imaging* online.

Funding

This work was supported by European Research Area Network on Cardiovascular Diseases (ERA-CVD, EMPATHY project), ProCardio Centre for Innovation supported by the Norwegian Research Council (grant #309762) and GENE POSITIVE grant #288438, and the Netherlands Organisation for Scientific Research (NWO-ZonMw, VID1 grant #016.176.340 to J.L., and NWO-ZonMw Off Road 2021 to A.S.J.M.t.R.). F.W.A. is supported by UCL Hospitals NIHR Biomedical Research Centre.

Conflict of interest: None declared.

Data availability

The data underlying this article cannot be shared due to the privacy of the individuals who participated in the study. The data will be shared upon reasonable request to the corresponding author

References

- Corrado D, Link MS, Calkins H. Arrhythmogenic right ventricular cardiomyopathy. *N Engl J Med* 2017 Jan 5;**376**:61–72.
- Groeneweg JA, Bhonsale A, James CA, te Riele AS, Dooijes D, Tichnell C et al. Clinical presentation, long-term follow-up, and outcomes of 1001 arrhythmogenic right ventricular dysplasia/cardiomyopathy patients and family members. *Circ Cardiovasc Genet* 2015;**8**:437–46.
- Calkins H, Corrado D, Marcus F. Risk stratification in arrhythmogenic right ventricular cardiomyopathy. *Circulation* 2017;**136**:2068–82.
- Cadrin-Tourigny J, Bosman LP, Nozza A, Wang W, Tadros R, Bhonsale A et al. A new prediction model for ventricular arrhythmias in arrhythmogenic right ventricular cardiomyopathy. *Eur Heart J* 2019;**40**:1850–8.
- Baudinaud P, Laredo M, Badenco N, Rouanet S, Waintraub X, Duthoit G et al. External validation of a risk prediction model for ventricular arrhythmias in arrhythmogenic right ventricular cardiomyopathy. *Canadian Journal of Cardiology* 2021;**37**:1263–6.
- Aquaro GD, de Luca A, Cappelletto C, Raimondi F, Bianco F, Botto N et al. Comparison of different prediction models for the indication of implanted cardioverter defibrillator in patients with arrhythmogenic right ventricular cardiomyopathy. *ESC Heart Fail* 2020;**7**:4080–8.
- Jordà P, Bosman LP, Gasperetti A, Mazzanti A, Gourraud JB, Davies B et al. Arrhythmic risk prediction in arrhythmogenic right ventricular cardiomyopathy: external validation of the arrhythmogenic right ventricular cardiomyopathy risk calculator. *Eur Heart J* 2022;**43**:3041–52.
- Protonotarios A, Bariani R, Cappelletto C, Pavlou M, García-García A, Cipriani A et al. Importance of genotype for risk stratification in arrhythmogenic right ventricular cardiomyopathy using the 2019 ARVC risk calculator. *Eur Heart J* 2022;**43**:3053–67.
- Carrick RT, te Riele ASJM, Gasperetti A, Bosman L, Muller SA, Pendleton C et al. Longitudinal prediction of ventricular arrhythmic risk in patients with arrhythmogenic right ventricular cardiomyopathy. *Circ Arrhythm Electrophysiol* 2022;**15**:e011207.
- Kirkels FP, Lie ØH, Cramer MJ, Chivulescu M, Rootwelt-Norberg C, Asselbergs FW et al. Right ventricular functional abnormalities in arrhythmogenic cardiomyopathy. *J Am Coll Cardiol Img* 2021;**14**:900–10.
- Lie ØH, Rootwelt-Norberg C, Deigaard LA, Leren IS, Stokke MK, Edvardsen T et al. Prediction of life-threatening ventricular arrhythmia in patients with arrhythmogenic cardiomyopathy: a primary prevention cohort study. *J Am Coll Cardiol Img* 2018;**11**:1377–86.
- Sarvari SI, Haugaa KH, Anfinson OG, Leren TP, Smiseth OA, Kongsgaard E et al. Right ventricular mechanical dispersion is related to malignant arrhythmias: a study of patients with arrhythmogenic right ventricular cardiomyopathy and subclinical right ventricular dysfunction. *Eur Heart J* 2011;**32**:1089–96.
- Leren IS, Saberniak J, Haland TF, Edvardsen T, Haugaa KH. Combination of ECG and echocardiography for identification of arrhythmic events in early ARVC. *J Am Coll Cardiol Img* 2017;**10**:503–13.
- Rootwelt-Norberg C, Lie ØH, Chivulescu M, Castrini AI, Sarvari SI, Lyseggen E et al. Sex differences in disease progression and arrhythmic risk in patients with arrhythmogenic cardiomyopathy. *Europace* 2021;**23**:1084–91.
- Mast TP, Teske AJ, Walmsley J, van der Heijden JF, van Es R, Prinzen FW et al. Right ventricular imaging and computer simulation for electromechanical substrate characterization in arrhythmogenic right ventricular cardiomyopathy. *J Am Coll Cardiol* 2016;**68**:2185–97.

16. Marcus FI, McKenna WJ, Sherrill D, Basso C, Bauce B, Bluemke DA et al. Diagnosis of arrhythmogenic right ventricular cardiomyopathy/dysplasia: proposed modification of the Task Force Criteria. *Circulation* 2010;**121**:1533–41.
17. Richards S, Aziz N, Bale S, Bick D, Das S, Gastier-Foster J et al. Standards and guidelines for the interpretation of sequence variants: a joint consensus recommendation of the American College of Medical Genetics and Genomics and the Association for Molecular Pathology. *Genet Med* 2015;**17**:405–24.
18. Voigt JU, Pedrizzetti G, Lysyansky P, Marwick TH, Houle H, Baumann R et al. Definitions for a common standard for 2D speckle tracking echocardiography: consensus document of the EACVI/ASE/industry task force to standardize deformation imaging. *Eur Heart J Cardiovasc Imaging* 2015;**16**:1–11.
19. Badano LP, Koliaas TJ, Muraru D, Abraham TP, Aurigemma G, Edvardsen T et al. Standardization of left atrial, right ventricular, and right atrial deformation imaging using two-dimensional speckle tracking echocardiography: a consensus document of the EACVI/ASE/industry task force to standardize deformation imaging. *Eur Heart J Cardiovasc Imaging* 2018;**19**:591–600.
20. Van Buuren S, Boshuizen HC, Knook DL. Multiple imputation of missing blood pressure covariates in survival analysis. *Stat Med* 1999;**18**:681–94.
21. White IR, Royston P, Wood AM. Multiple imputation using chained equations: issues and guidance for practice. *Stat Med* 2011;**30**:377–99.
22. Rubin DB. *Multiple Imputation for Nonresponse in Surveys*. New York: John Wiley and Sons; 1987.
23. Corrigendum to: a new prediction model for ventricular arrhythmias in arrhythmogenic right ventricular cardiomyopathy. *Eur Heart J*. 2022;**43**:2712.
24. Bosman LP, Sammani A, James CA, Cadrin-Tourigny J, Calkins H, van Tintelen JP et al. Predicting arrhythmic risk in arrhythmogenic right ventricular cardiomyopathy: a systematic review and meta-analysis. *Heart Rhythm* 2018;**15**:1097–107.
25. Borgquist R, Haugaa KH, Gilljam T, Bundgaard H, Hansen J, Eschen O et al. The diagnostic performance of imaging methods in ARVC using the 2010 Task Force Criteria. *Eur Heart J Cardiovasc Imaging* 2014;**15**:1219–25.
26. Kirkels FP, Bosman LP, Taha K, Cramer MJ, van der Heijden JF, Hauer RNW et al. Improving diagnostic value of echocardiography in arrhythmogenic right ventricular cardiomyopathy using deformation imaging. *J Am Coll Cardiol Img* 2021;**14**:2481–83.
27. Taha K, Kirkels FP, Teske AJ, Asselbergs FW, van Tintelen JP, Doevendans PA et al. Echocardiographic deformation imaging for early detection of genetic cardiomyopathies: JACC review topic of the week. *J Am Coll Cardiol* 2022;**79**:594–608.
28. Haugaa KH, Basso C, Badano LP, Bucciarelli-Ducci C, Cardim N, Gaemperli O et al. Comprehensive multi-modality imaging approach in arrhythmogenic cardiomyopathy —an expert consensus document of the European Association of Cardiovascular Imaging. *Eur Heart J Cardiovasc Imaging* 2017;**18**:237–53.
29. Taha K, Mast TP, Cramer MJ, van der Heijden JF, Asselbergs FW, Doevendans PA et al. Evaluation of disease progression in arrhythmogenic cardiomyopathy: the change of echocardiographic deformation characteristics over time. *J Am Coll Cardiol Img* 2020;**13**:631–34.
30. te Riele ASJM, James CA, Philips B, Rastegar N, Bhonsale A, Groeneweg JA et al. Mutation-positive arrhythmogenic right ventricular dysplasia/cardiomyopathy: the triangle of dysplasia displaced. *J Cardiovasc Electrophysiol* 2013;**24**:1311–20.
31. Mast TP, Taha K, Cramer MJ, Lumens J, van der Heijden JF, Bouma BJ et al. The prognostic value of right ventricular deformation imaging in early arrhythmogenic right ventricular cardiomyopathy. *J Am Coll Cardiol Img* 2019;**12**:446–55.
32. Aquaro GD, de Luca A, Cappelletto C, Raimondi F, Bianco F, Botto N et al. Prognostic value of magnetic resonance phenotype in patients with arrhythmogenic right ventricular cardiomyopathy. *J Am Coll Cardiol* 2020;**75**:2753–65.
33. Tower-Rader A, Mohanane D, To A, Lever HM, Popovic ZB, Desai MY. Prognostic value of global longitudinal strain in hypertrophic cardiomyopathy. *J Am Coll Cardiol Img* 2019;**12**:1930–42.
34. Kawakami H, Nerlekar N, Haugaa KH, Edvardsen T, Marwick TH. Prediction of ventricular arrhythmias with left ventricular mechanical dispersion. *J Am Coll Cardiol Img* 2020;**13**:562–72.